



Modeling nitrous oxide emissions from agricultural soil incubation experiments using CoupModel

Jie Zhang¹, Wenxin Zhang², Per-Erik Jansson³, Søren O. Petersen¹

¹Department of Agroecology, iClimate, Aarhus University, Tjele, Denmark

5 ²Department of Physical Geography and Ecosystem Science, Lund University, Lund, Sweden

³Department of Sustainable Development, Environmental Science and Engineering, KTH Royal Institute of Technology, Stockholm, Sweden

Correspondence to: Jie Zhang (jiezhang@agro.au.dk)

Abstract. Efforts to develop effective climate mitigation strategies for agriculture require methods to estimate nitrous oxide (N₂O) emissions from soil. Process-based biogeochemical models have been used for such estimations but were mainly tested with field-scale measurements. In this study, results from a short-term (43-day) factorial incubation experiment were used to investigate the ability of a process-oriented model (CoupModel) to estimate N₂O and carbon fluxes, and soil mineral nitrogen (N) dynamics. This study identified the sensitivities of model parameters when estimating three output variables using a global sensitivity analysis approach. Our results suggested that important parameters regarding N₂O flux estimates were linked to the decomposability of soil organic matter (e.g. organic C pool sizes) and the denitrification process (e.g. Michaelis constant and denitrifier respiratory rates). The model was able to simulate low-magnitude daily and cumulative N₂O fluxes with model errors (MEs) close to zero, but tended to underestimate N₂O fluxes as observed daily values increased over 0.1 g N m⁻² day⁻¹. Besides, the response of N₂O emissions to soil moisture was not well reflected in the model, probably related to the indirect involvement of soil moisture response function in the denitrification process. We also evaluated ancillary variables regarding N cycling, which indicates that more frequent measurements and additional types of observed data such as soil oxygen content and the microbial sources of emitted N₂O are required to further evaluate model performance and biases. The current description of the N cycling process in the model may not consistently represent the temporal scale of nitrification and denitrification processes behind N₂O emissions. The major challenges for calibration are associated with high sensitivities of denitrification parameters to initial soil moisture abiotic conditions and residue amendment. For the development of process-based models, we suggest there is a need to address soil heterogeneity, and to revisit current subroutines of moisture response functions.

1 Introduction

The potent greenhouse gas nitrous oxide (N₂O) has been estimated to be responsible for about 7 % of the overall global radiative forcing by long-lived greenhouse gases (World Meteorological Organization, 2021). N₂O emissions from the agricultural sector account for 60-70 % of the total anthropogenic emissions of this gas (Davidson and Kanter, 2014; Syakila



and Kroeze, 2011). To provide a scientific basis for developing achievable climate mitigation strategies, improved understanding of N₂O production in agricultural soils and quantification of N₂O emissions are urgently needed.

35 N₂O emissions from agricultural soils are driven by a suite of microbiological processes among which nitrification and denitrification predominate as sources of N₂O. The factors directly regulating nitrification and denitrification activity are the availability of mineral nitrogen (N), oxygen, and degradable carbon (C) sources used by denitrifying organisms (Wijler and Delwiche, 1954). Indirect controls include soil temperature, moisture, pH, and soil texture. During nitrification, where ammonia (NH₃, at equilibrium with ammonium NH₄⁺) is oxidized to nitrate (NO₃⁻), a small proportion of N may be lost as N₂O (Firestone and Davidson, 1989). Nitrification mainly occurs in well-aerated soils with moderate water content (Goreau et al., 1980; Li et al., 1992; Parton et al., 1996). In contrast, denitrification is a microbial process that occurs under anaerobic
40 conditions where NO₃⁻ is reduced to gaseous N. Soil C substrates are electron donors for denitrification, but they are also a sink for oxygen that leads to anaerobic microsites (Sommer et al., 2004), and finally NO₃⁻ is used as electron acceptors. Nitrifying and denitrifying bacteria are most active to produce N₂O in environments with abundant N relative to assimilatory demands by other microorganisms or plants (Firestone and Davidson, 1989), as is often the case following input of fertilizers, manure, or crop residues to the soil.

45 Farming practices influence the potential for interactions between microbial, physical, and chemical processes in the soil. Incorporation of crop residues can reduce NH₃ losses and enhance degradation compared to leaving residues at the soil surface, but the increased soil water holding capacity and oxygen demand locally may stimulate the development of anaerobic microsites and bacterial denitrification activity (Kravchenko et al., 2018; Kuzyakov and Blagodatskaya, 2015). Mechanical disturbance via tillage may influence soil properties (e.g. porosity, aggregate size distribution, solute and gas diffusivities) and microbial enzyme activities, with subsequent changes in the magnitude of N₂O emissions (Grandy and
50 Robertson, 2006).

The quantification of N₂O emissions from agroecosystems is constrained by logistical challenges and resource availability (e.g. analytical equipment and budgets). Process-oriented biogeochemical models, e.g. DNDC (Li et al., 1992), DayCent (Parton et al., 1996), APSIM (Keating et al., 2003), and CoupModel (Jansson and Moon, 2001), have been developed to
55 partly compensate for these limitations. In the application of process-based models, available in-situ measurements can be used to infer model parameters and allow simulation of soil N transformations and N₂O emissions at temporal and spatial scales beyond the monitoring sites, but accurately simulating the magnitude and temporal variability of N₂O fluxes under contrasting contexts still poses a challenge. Those models may provide reasonable estimates of N₂O emissions from soils in a narrow context, usually at specific sites and at annual time scales, but they become less successful at finer time resolution
60 (e.g. diurnal time steps) and at sites different from the pre-calibrated ones. This represents a barrier in evaluating the effects of agricultural land use and management on greenhouse gas emissions (Brilli et al., 2017). Such model errors are often attributed to physical and biogeochemical processes being inadequately represented, which calls for the improvement of



process descriptions beyond parameter optimization (Abdalla et al., 2010; Brilli et al., 2017; Gaillard et al., 2018; Uzoma et al., 2015).

65 Process models attempt to reproduce the most relevant physical and biogeochemical processes through understanding
grounded in the best available theory at the time they were developed, after which some new empirical adjustments were
gradually added. CoupModel, used in the current investigation, has a high level of detail on soil physical and abiotic
components and has adopted details of submodules of nitrification, denitrification, and gas fluxes from the DNDC model (Li
et al., 2000; Norman et al., 2008). The description of N₂O emissions, including the links between soil environmental factors
70 and biological reactions, is based on a series of hypotheses and results generated from both field measurements and
laboratory incubations studies (Li et al., 2000), and the algorithms and parameterization of microbial growth and death
dynamics were specifically supported by the latter. While our understanding regarding decomposition and denitrification has
advanced in recent decades, the incorporation of state-of-the-art knowledge into process-based models has lagged behind. To
test the description of N₂O emissions, it is necessary to apply the model to results from properly controlled laboratory
75 experiments, where the impact of ill-defined pedo-climatic conditions on model predictability can be minimized (Brilli et al.,
2017). This may reveal causal relationships behind gas production and transport in a microcosm representing the ecosystem,
and suggest new paths for model development.

The application of process-based models has often been challenged by the paucity of prior information and measurements
compared to the model's demands, and this is also the case when applying a model to incubation experiments. One widely-
80 used model calibration method to bridge the gap between model requirements and available data, and to quantify parameter
uncertainties, is "generalized likelihood uncertainty estimation (GLUE)" (Beven and Binley, 1992). During model
calibration, uncertainty analysis can help assess whether the model performance is good enough compared to the
requirement of the applied use of the model, and to evaluate possible biases in simulations (U.S. Environmental Protection
Agency, 2009). This may be facilitated by applying a Global Sensitivity Analysis (GSA), which can rank the sensitivities of
85 parameters so that the model calibration can focus on the relatively more sensitive parameters (Vezzaro et al., 2012), and
thereby the model's uncertainties can be more efficiently constrained. While model processes and performance have been
extensively documented, in many studies N₂O emissions alone were used to train and test the subroutines of nitrification and
denitrification (Chen et al., 2008). Evaluation under controlled conditions and with ancillary measurements is noticeably
lacking, which makes it difficult to identify model structure limitations. Thus, a first step in understanding model
90 performance may be an evaluation using new datasets that contain different variables linked to N cycling based on targeted
laboratory experiments. To our knowledge, no previous study has attempted a systematic sensitivity and uncertainty analysis
in the prediction of N₂O emissions based on laboratory incubation results.

For this work, we selected CoupModel which has integrated options for uncertainty estimation and performance evaluation
(Jansson, 2012). It has a flexible setting of soil layer thickness down to a scale of mm, which is proper to study soil physical



95 processes at the scale of incubation experiments. Data sets used in the model were obtained from a 43-day laboratory
incubation using a factorial-based design with various crop residue practices and abiotic factors (Taghizadeh-Toosi et al.,
2021). Specifically, our objectives were (i) to conduct a global sensitivity analysis for parameters in a model setup that can
simulate N cycling under different incubation treatments (ii) to calibrate the model and quantify the uncertainty in the
estimates of N₂O emissions, and (iii) to discuss any model limitations identified and suggest directions for future model
100 improvement. We hypothesized that the model is able to simulate the daily and cumulative N₂O emissions under contrasting
environments in incubated soil cores. Furthermore, we hypothesized that it would be difficult to constrain the parameters of a
complex model to an unambiguous solution with limited laboratory measurements.

2 Materials and methods

2.1 Laboratory incubation experiment

105 In spring 2018, soil used for the experiment was collected from the 0-20 cm tilled layer at the Lönnstorp Field Station,
Sweden. Red beets had been grown in the previous year with no cover crop during winter. The soil is sandy loam (61.8 %
sand, 22.4 % silt, and 15.8 % clay) with a pH of 6.18, C content of 15 g kg⁻¹, and N content of 1.49 g kg⁻¹. After collection,
the soil was partially dried, stored at -20 °C, and thawed one day before sieving and use for the experiment.

Treatments were prepared with four different soil conditions regarding the moisture level (i.e. 40 or 60 % WFPS) and nitrate
110 content (i.e. no nitrate addition or addition of KNO₃ to 100 mg NO₃⁻-N kg⁻¹ dry wt. soil). Soil cores were prepared by
stepwise packing 1 cm layers of soil to a density of 1.25 g cm⁻³ in cylinders to the height of 8 cm, at each step adding
deionized water or a KNO₃ solution. The soil treatments were pre-incubated for one week at 15 °C. The experiment involved
two different crop residues, red clover (RC) and winter wheat (WW). RC residues had a C/N ratio of 17.9, and a moisture
level corresponding to 80 % of the fresh weight. The WW residues had a C/N ratio of 90.9, and the moisture content
115 corresponded to 20 % of the fresh weight. WW residues had a higher proportion of lignin and ash (11.7 %) than RC residues
(5.1 %). In the experiment, RC or WW residues were either mixed at a rate of 0.04 g DM cm⁻² into the soil from 0-4 cm
depth and then repacked, or residues were placed as a layer at 4 cm depth; only results from the mixed treatments were used
in the present study. Incubations with RC and WW took place sequentially, and therefore each residue treatment had its own
set of unamended controls. Thus, in total 16 treatments from the incubation experiment were used for this modeling study,
120 including unamended soils (as controls) and soil-residue mixtures from either red clover or winter wheat.

All cylinders were covered at both ends with perforated plastic caps and incubated at 15 °C for up to 43 days. Gas sampling
for N₂O and CO₂ flux measurements took place ten times, i.e., on day 1, 3, 6, 9, 13, 16, 22, 29, 36, and 43. Gas
concentrations were determined by gas chromatography. Additionally, nitric oxide (NO) fluxes were quantified in four
selected treatments set up separately. Soil mineral N pools in all treatments were measured at four destructive samplings

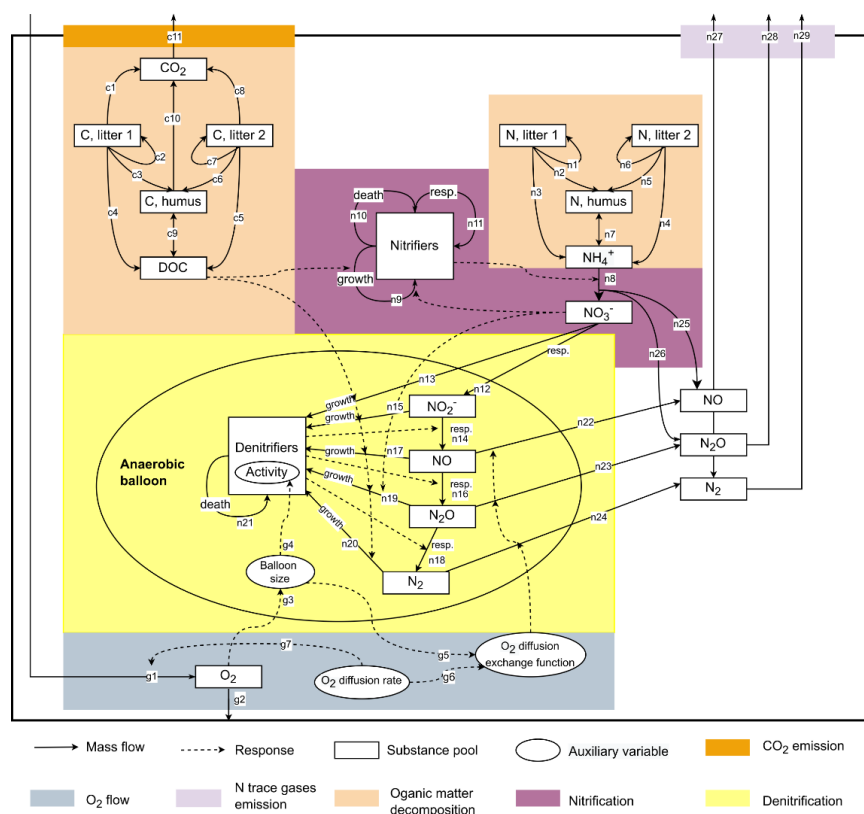


125 after 1, 6, 22, and 43 days of incubation. Further details about the experimental treatments, preparations, and analytical
 methods are given by Taghizadeh-Toosi et al. (2021).

2.2 Model description and simulation setup

2.2.1 CoupModel

130 This study used CoupModel v6.1, which can be downloaded from <http://coupmodel.com>. A detailed description of
 CoupModel can be found in Jansson & Karlberg (2010). The main structure of the model is a one-dimensional vertical soil
 profile with user-defined layer thickness and subdivisions. The current setup of CoupModel includes a number of
 components, of which the following are linked to N₂O emissions (Fig. 1): (i) soil organic matter (SOM) decomposition and
 mineralization; (ii) nitrification and nitrifier growth; (iii) denitrification and denitrifier growth; and (iv) gas diffusion
 135 between soil layers and internal exchange of N trace gases between aerobic and anaerobic micro-sites. In the nitrification
 subroutine, CoupModel accounts for response functions of soil temperature, soil moisture, mineral N concentration, and pH.
 For denitrification, each step in the chain of denitrification is explicitly calculated, and denitrifier activity is directly
 influenced by soil temperature, pH, nitrogen oxides and anaerobic fraction. The anaerobic soil volume fraction is calculated
 using the “anaerobic balloon” concept, as implemented in the DNDC model (Li et al., 2000; Norman et al., 2008).





140 **Figure 1: A conceptual diagram of major C and N processes in the current setup of CoupModel. The details of parameters and equations in each C or N process can be found in Table S2.**

2.1.2 Simulation settings

The modeled soil profile consisted of a single soil layer with a depth of 4 cm for the control treatments and 4.2 cm for the mixed treatments, allowing a 2 mm increment owing to residue amendment as observed in the experiment. We only
145 simulated the upper half of the 8 cm soil core since the model only allows external gas exchange at the upper boundary of the soil profile, although in the experiments both ends of the cylinder were exposed to air and the two halves were identical for control soils. For the water process, it was assumed that there was no evaporation from the surface and no vertical water flow across the lower boundary. Constant temperature was set for the upper and lower boundaries, in accordance with incubation conditions. The model was initialized based on the measured soil water content, temperature, pH, total organic C
150 and N, and NO_3^- -N, and NH_4^+ -N of the incubated soil cores. The dynamics of SOM dynamics were simulated with first-order kinetics using three pools (litter1, litter2, and humus). Considering there were no explicit pools designed for crop residue addition, we assigned the rapidly decomposable SOM and metabolic residue materials (e.g. sugars and proteins) to litter1, the moderately decomposable SOM and structural residue materials (e.g. lignin and other fibers) to litter2, and the resistant SOM to humus. For simulating gas transport, we selected the steady-state mode where the oxygen content within the soil
155 profile is a trade-off between soil oxygen consumption and diffusive supply from surface air, and N trace gases are directly lost to the ambient air from the layer in which they are generated.

Calibration datasets – Measurements used for model calibration were N_2O flux, CO_2 flux, NO flux, NO_3^- -N content, and NH_4^+ -N content. As the gas fluxes and mineral N content in the upper part with soil-residue mixtures and the lower part with bulk soil were not analyzed separately, we assumed that soil C and N turnover in the lower, unamended part was identical to
160 that of control treatments to create datasets for the residue-amended part for modeling. Specifically, the amounts of mineral N and gas fluxes recorded on individual sampling days in the controls were divided by two and subtracted from the values recorded in residue-amended soil.

Initial values – (1) Mineral N: Since the mineral N content in the unamended control soil changed little during incubation and the mineral N content in crop residues was negligible, the initial NH_4^+ -N and NO_3^- -N values for the control and residue-
165 amended treatments were taken as the measurement in control soil on day 1. (2) Soil moisture: For the control treatments, the initial volumetric water content was calculated from the water-filled pore space (WFPS) levels of 40 or 60 % according to the total porosity of 0.53. For the residue treatments, the initial volumetric water content was calculated from the moisture content of soil and crop residues (Taghizadeh-Toosi et al., 2021). (3) Organic matter pools: The partitioning of soil organic C between litter1, litter2, and humus was defined by the ratio 0.02:0.54:0.44 (Gijssman et al., 2002). For crop residues, the
170 metabolic fraction of organic C was calculated from the lignin/N ratio: Metabolic fraction = $0.85 - 0.013 (\text{lignin}/\text{N})$ (Gijssman



et al., 2002), and hence the organic C allocation between litter1 and litter2 had a ratio of 0.82:0.18 for RC and 0.55:0.45 for WW. The allocation of organic N in different pools followed the pattern of C and the C/N ratios (Table S5).

A summary of calibration data sets can be found in Table S1 in the supplement, in which cumulative gas emissions were estimated by linearly interpolating between sampling dates and integrating the area under emission curves; and average mineral N were calculated by dividing the integrated values by the sampling period. The results for nitrate in soil cores with residues were not included due to high uncertainty in the calculations that was probably caused by solute transport between the unamended and amended soil layers, as observed in a related incubation experiment using some of the same soil and residue treatments conducted by Lashermes et al. (2021).

2.3 Model sensitivity and uncertainty analysis

2.3.1 Global sensitivity analysis

Given uncertain prior information, the study used Morris screening (Morris, 1991) for a global sensitivity analysis to identify the most important input parameters and process parameters affecting N₂O fluxes. We included seven input parameters related to the characteristics of soil and crop residues (i.e. soil porosity, residue porosity, soil pH, and sizes of organic C pools), with realistic ranges of uncertainty intervals considered. Besides, we considered 45 process parameters involved in the relevant model processes. These parameters are listed in Table S4.

The Morris screening method is a commonly used sensitivity analysis technique, based on an efficient sampling strategy for performing a randomized calculation of one-factor-at-a-time (OAT) sensitivity analysis. This method can be viewed as a compromise between a simple OAT approach and the more complex GSA methods (e.g. variance-based approaches) as it provides a good approximation to the global sensitivity measure of the parameters at an affordable computational cost.

Furthermore, it was considered excessive and unnecessary in the present study to adopt a more detailed analysis given the limited data availability.

The elementary effect (EE) was estimated by comparing the variation of the model's output y^j , with the variation of a given parameter θ_i , according to Eq. (1). The number of iterations n was set to 50, and the optimal perturbation factor Δ was set to 2/3 by dividing the input space into four levels (Morris, 1991). To allow comparison across outputs, the EE was then standardized by using the standard deviation of the model factor and the standard deviation of the output (SEE, Eq. (2)). The significance of the impact of parameters was tested by comparing the mean of the SEE of those parameters to twice the standard error (*sem*, Eq. (3)) (Sin et al., 2009). If the input factor lies outside this range, it is said to have a significant effect on the output. The codes used in the analysis were adapted from (Sin et al., 2009).



$$EE_i^j = \frac{y(\theta_1^j, \theta_2^j, \dots, \theta_i^j + \Delta_{OPT}, \dots, \theta_{m-1}^j, \theta_m^j) - y(\theta_i^j)}{\Delta} \quad (1)$$

$$SEE_i^j = EE_i^j \cdot \frac{\sigma_{\theta_i}}{\sigma_y} \quad (2)$$

$$sem_i = \pm \frac{\sigma(SEE_i^j)}{\sqrt{n}} \quad (3)$$

200 The GSA was performed to the model-evaluation measure root mean square error (RMSE) for three variables: N₂O flux, CO₂ flux, and soil NH₄⁺ which had relatively complete measurement data sets. By applying the sensitivity analysis to the likelihood measure, the main factors that drive the model runs with a good fit to data could be identified (Ratto et al., 2001). The results from sensitivity analyses were further used to identify process parameters for inclusion in the uncertainty analysis due to their contribution to output variability.

2.3.2 Uncertainty analysis

205 Model calibration was conducted separately for each of the 16 treatments to give more flexibility in model parameterization. The calibration was carried out with reference to five measurement variables, namely N₂O flux, CO₂ flux, NH₄⁺ content, NO₃⁻ content, and NO flux (only four treatments), using the “generalized likelihood uncertainty estimation” (GLUE) technique (Beven and Binley, 1992). The GLUE method does not seek the single best fit to the measured data but utilizes an ensemble of model simulations that represent equally good results using informal likelihood measures, often mentioned as
210 acceptance criteria. In this study, we first described the entire ensemble of model runs as prior runs and after applying selection criteria the selected ensemble of model runs was analyzed as posterior runs or behavioral runs. Based on the calculated sensitivity indices from Morris screening, a total of 26 process parameters were selected for calibration where the parameters with marginal SEEs were omitted and only one denitrifier growth parameter was kept in each step of the denitrification chain (see Table S4). These parameters were uniformly or log-uniformly distributed within the predefined
215 ranges, from which 20,000 parameter sets were then randomly sampled for model runs. Out of these runs, whether a parameter set was accepted or not was based on the defined criteria, which in this study consisted of coefficient of determination, R² and mean error, ME. The latter is defined as ME = E (O_i - S_i), where S_i and O_i are the time series of the simulated and observed data.

220 The ME acceptance threshold of each variable was set to be around the average of daily measurements taking into account the different magnitudes of each variable (see Table S3). In prior runs ME values were often skewed to one side (above 0 or below 0) while setting the same threshold on both sides rejected most of the prior model runs, and hence the ME criterion on one side might be looser than the other. For N₂O emissions with marked peak fluxes, a combination of R² and ME was used for the selection of posterior parameters to simulate the dynamics and magnitudes. An ensemble of ca. 50 posterior runs was



225 selected with an acceptance rate of 0.25% based on prior simulations. The uncertainties of model predictions were quantified within the limits and posterior probability distributions of parameters.

230 Finally, to investigate whether the treatment effects concerning soil moisture and nitrate level could be represented by a common parameterization, we attempted to calibrate process parameters against combined data sets from multiple treatments where measurements from every four treatments with the same residue application were pooled. The prior parameter ensembles used the same 20,000 parameter sets as the single-treatment calibration. Accordingly, the measurement datasets from the four treatments in each group were pooled and thus a larger data set for model evaluation was obtained. The procedure of selecting behavioral runs followed the aforementioned approach based on ME and R^2 . A diagram that describes the analysis workflow for this study is presented in Fig. 2.

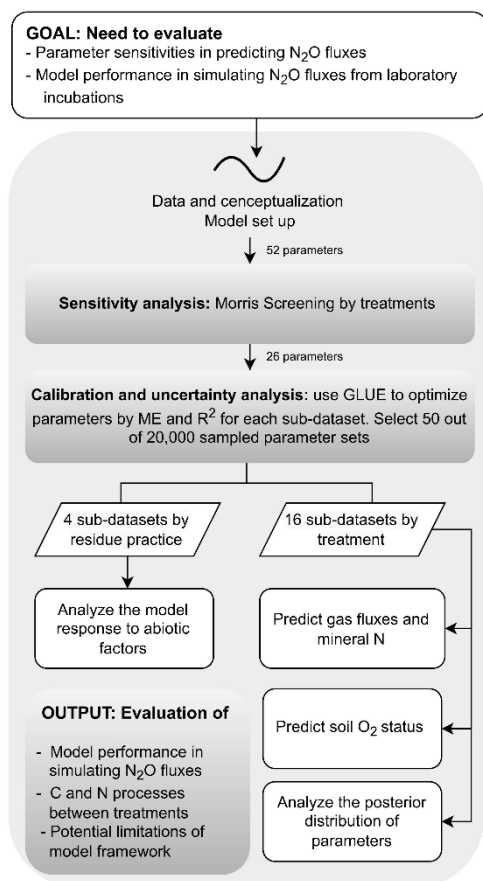


Figure 2: A schematic diagram for performing sensitivity and uncertainty analyses.

235 **3 Results**



3.1 Sensitivity analysis

The results of Morris screening were evaluated by comparing the absolute SEE concerning N₂O flux, CO₂ flux, and soil NH₄⁺ for individual treatments. Figure 3a-c lists all parameters ranking in the top five across the 16 treatments. Parameter ranking was performed based on the absolute mean of SEEs – the higher the absolute value, the more important the parameter is, as shown by the shade of color in Fig. 3a-c. In general, the parameters identified as most influential for soil respiration (CO₂ flux) and NH₄⁺ content showed robustness across treatments as they differed only slightly in their ranking with, respectively, eight and nine different parameters represented. In contrast, more inter-treatment variation was found in the parameter ranking for N₂O emissions with 18 different parameters represented. For N₂O, the parameters exhibiting relatively high SEE values for most treatments belonged to categories of SOM decomposition and denitrification (Table S2), including d_{effNO} , SOC_h , $d_{growthNO_3}$, cn_m , and $d_{hrateN_xO_y}$. The model input, SOC_h , characterizing the partitioning of SOM pools in the simulation, was found to be crucial in 13 out of 16 treatments. d_{effNO} represents the respiration of denitrifying bacteria based on NO, and it showed relatively large elementary effects for almost all treatments by directly regulating the reduction step from NO to N₂O. The parameter $d_{growthNO_3}$ describes the loss of NO₃⁻ from the anaerobic nitrogen pool due to microbial growth. $d_{hrateN_xO_y}$ represents the N concentration for half rate in the denitrification process and is also known as the Michaelis constant of the enzyme (see n13, n15, n17, n19, and n20 in Fig. 1).

Parameters that had the greatest impact on CO₂ emissions were concentrated in the following: SOC_h , SOM decomposition rates (k_{l2} , k_{l1}), and the corresponding efficiencies ($f_{e,l2}$, $f_{e,l1}$). In addition, the two parameters, $p_{\theta Low}$ and θ_{wilt} , controlling the lower limit of the soil moisture response function for the decomposition of organic matter (see Eq. (5.86) in Table S2), exhibited distinct influences for the treatments at the lower moisture level.

The main processes influencing the NH₄⁺ content of the soil were identified as SOM decomposition and denitrification, and influential parameters included: cn_m , SOC_h , k_{l2} , and $f_{e,l2}$. The C/N ratio of microbes, cn_m , has an influence on the mineral N content by changing the magnitude and direction of soil mineralization/immobilization of nitrogen (see n1-n7 and n11 in Fig. 1). It was also found that soil porosity (θ_s) had significant effects on some treatments, especially under higher moisture conditions. Besides, as a key intermediate of mineral nitrogen turnover, the content of NH₄⁺, was also influenced by denitrification-related parameters, such as $d_{growthNO_3}$.

The average elementary effects across all treatments are shown in Fig. 3d-f. For the N₂O flux, all parameters were located inside the wedge indicating that none of these parameters showed a significant effect across all treatments despite their significance in individual treatments. In contrast, we found that the other two variables, CO₂ flux, and NH₄⁺ content, were significantly affected by 15 and 28 parameters respectively. Moreover, all parameters showed non-linear effects on the outputs as revealed by their non-zero standard deviations, which suggested that simulated C and N processes did not solely depend on individual parameters but also their interactions.

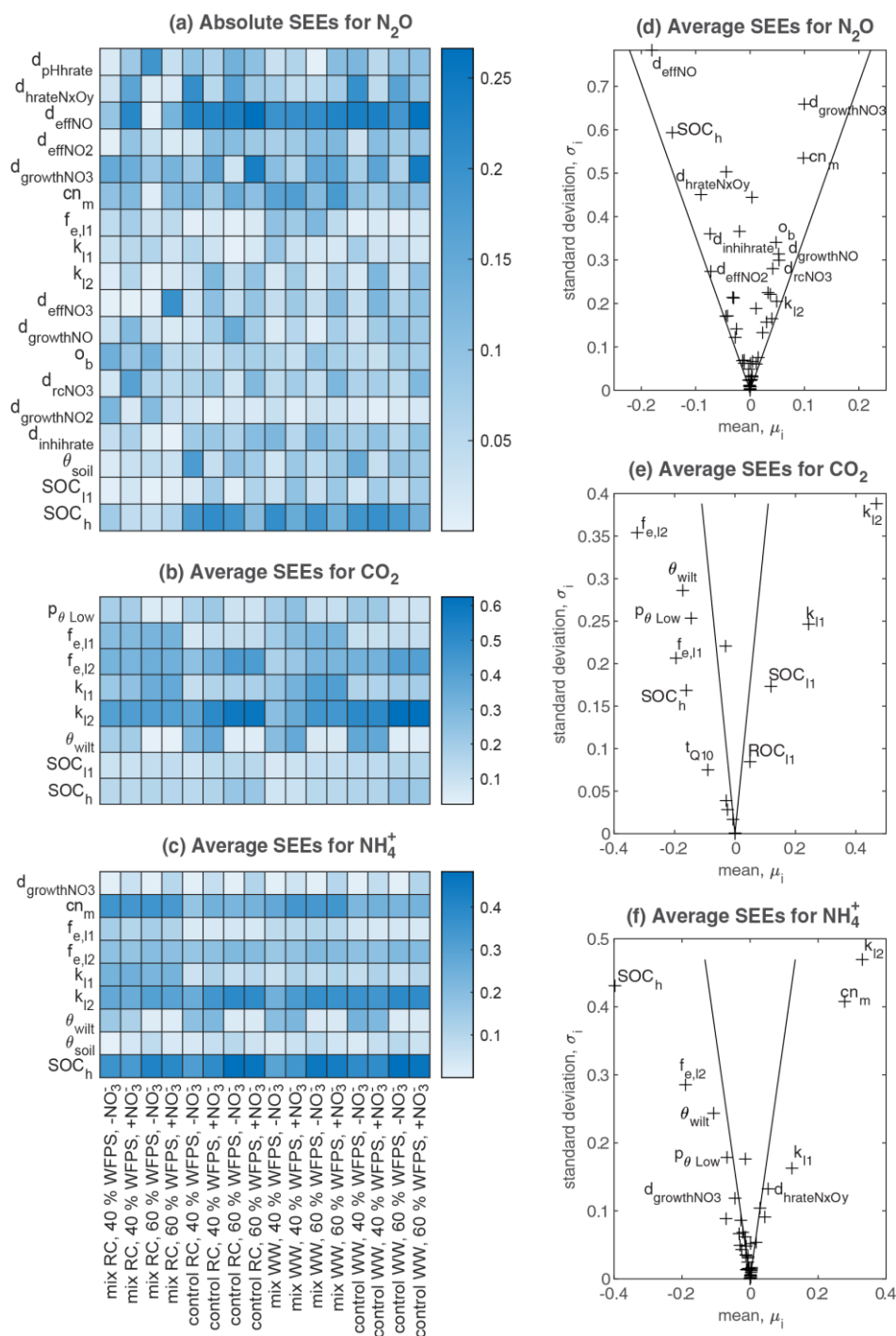


Figure 3: Sensitivity analyses for N₂O flux, CO₂ flux, and soil NH₄⁺ content in all treatments. (a-c): Heatmaps that include all parameters ranked in the top five places for each treatment based on absolute standardized elementary effects (SEEs). (d-f): Estimated mean and standard deviation of SEEs averaged across the 16 treatments, where the two lines drawn in each subplot



correspond to twice the standard error (sem): $\mu_i = \pm 2sem_i$ (see Sect. 2.3.1): if a factor is located inside the wedge, it indicates that its impact on the output is insignificant and vice versa.

3.2 Uncertainty analysis

3.2.1 Temporal dynamics of N₂O flux, CO₂ flux, and mineral N

275 In the experimental treatments with RC amendment, N₂O emission rates were consistently low at 40 % WFPS but were markedly higher and peaked on day 3 at 60 % WFPS (Fig. 5a). The highest measured daily N₂O flux was 1.4 g N m⁻² day⁻¹ in the RC treatment with NO₃⁻ addition at 60 % WFPS. Similar patterns were observed for CO₂ emission rates, with emission peaks at an early stage of incubation (day 1 or day 3) and then followed by a decline. In treatments amended with WW, N₂O evolution rates were generally low compared to those with RC amendment, and showed higher rates at 60 % WFPS and in
280 NO₃⁻ amended soil but treatment effects were generally minor. For CO₂ evolution, higher rates were detected by day 1, but there was also a secondary peak after 1-2 weeks. The control treatments of the WW residue incubations showed less CO₂ and N₂O release compared to the control treatments of the preceding RC incubations.

The prior models generally showed significantly biased mean errors in terms of gas emissions and soil mineral N, and their magnitude was reduced in the posterior models for most model outputs (Fig. 4a-d). For N₂O fluxes, most treatments
285 amended with WW and corresponding controls did not show significant deviations from the observed fluxes. In contrast, in treatments amended with RC and corresponding controls, though the absolute MEs had been reduced, there were still significant deviations generally in the direction of underestimating the observed fluxes. For CO₂ emissions, 13 out of 16 treatments showed reduced mean errors in the behavioral models and half of the treatments showed insignificant deviations from the observed fluxes. For soil NH₄⁺ content, there was a severe overestimation for most prior models, but this was
290 alleviated by posterior models, and seven treatments showed insignificant deviations from 0 after model calibration. For soil NO₃⁻ content in control treatments, the ME ranges of posterior runs were around zero while negative or positive biases existed especially the former. The simulated evolution of associated variables is depicted in Fig. 5a-d and results are summarized below.

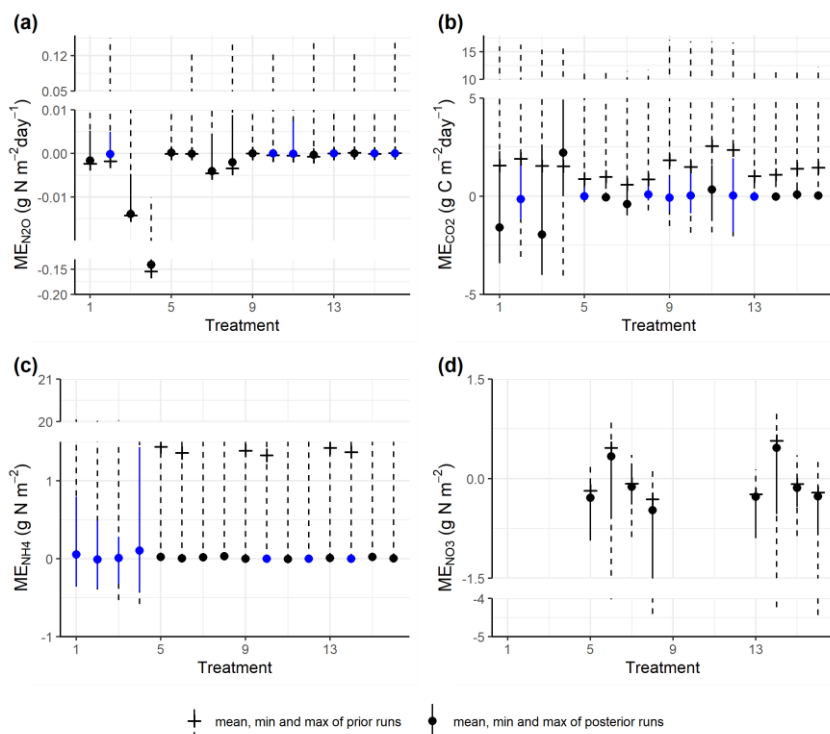
N₂O – The accepted simulations (Fig. 5a) were able to represent the scenarios with low daily N₂O emissions (10⁻⁵-10⁻² g N
295 m⁻² day⁻¹), while simulations failed to capture the large emission peaks (e.g. 1.4 g N m⁻² day⁻¹ and 0.13 g N m⁻² day⁻¹ for the two RC treatments with NO₃⁻ amendment), or the emission dynamics were reasonably simulated (e.g. R² > 0.4, see Table S3) but the peak values were lower than observed. The N₂O fluxes obtained from the model tended to increase over time and generally agreed with the observed fluxes in the second part of the experiment.

CO₂ – Overall, the behavioral models mimicked the measured dynamics and magnitude of CO₂ emissions well (Fig. 5b).
300 There were overestimations or underestimations by the model, most pronounced in the early stage of incubation. By day 14, a second peak of respiration was observed for the WW treatments that was not simulated by posterior models.



305 NH_4^+ – For RC residue treatments, net N mineralization was observed from the early to mid-stage of the incubation period, followed by a declining trend, whereas in the posterior models in three of four treatments the simulated NH_4^+ predicted a trend of net N mineralization throughout the incubation (Fig. 5c). Such a continuously increasing trend also existed in the prior runs, which would not be radically altered in the behavioral models by setting a stricter selection criterion for R^2 . For WW residue and control treatments the measured NH_4^+ content was at the detection limit, and the magnitude of the simulated NH_4^+ content was either in line with the measurements, or a bit higher.

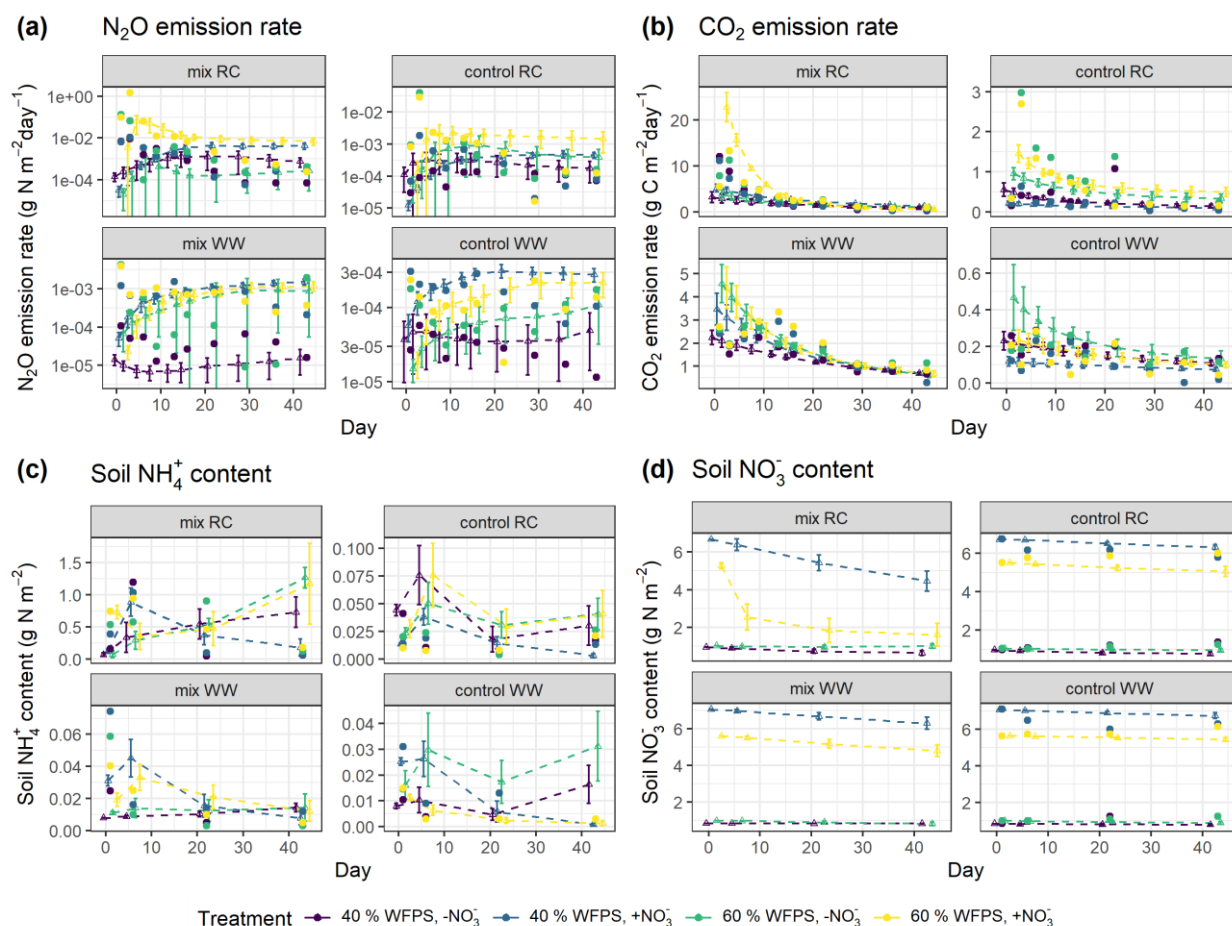
310 NO_3^- – The change of simulated daily NO_3^- content generally showed a declining trend for all control treatments, with modeled values comparable to observed data. While in most of the control treatments except for the ones with high moisture and NO_3^- amendment, the observed NO_3^- levels remained stable or slightly increased during incubation (Fig. 5d). For the treatments amended with crop residues, the simulated NO_3^- content showed a more clear downward trend throughout the period, consistent with NO_3^- being utilized as a substrate of denitrification in the simulation. Though no explicit measurement of NO_3^- within the residue-amended layer in the present experiment, the average NO_3^- within the entire soil core in RC treatments showed net consumption followed by a rebound (Taghizadeh-Toosi et al., 2021), consistent with observations for the RC-amended layer in a comparable incubation experiment by Lashermes et al. (2021). In view of this, 315 the simulated NO_3^- content in residue treatments exhibiting a continuous decline was probably lower than the actual values.





320

Figure 4: Comparison of the ME ranges between prior simulations and accepted simulations for daily N₂O fluxes (a), CO₂ fluxes (b), soil NH₄⁺ content (c), and soil NO₃⁻ content (d). Blue color shows ME values not significantly different from zero by one-sample *t*-tests (significance level $\alpha = 0.05$). Treatment indices 1-4 represent treatments of mix RC, 5-8 for control RC, 9-12 for mix WW, and 13-16 for control WW, where treatment conditions are, in order: “40% WFPS, -NO₃”, “40% WFPS, +NO₃”, “60% WFPS, -NO₃”, and “60% WFPS, +NO₃”. No measured data for nitrate in residue treatments.



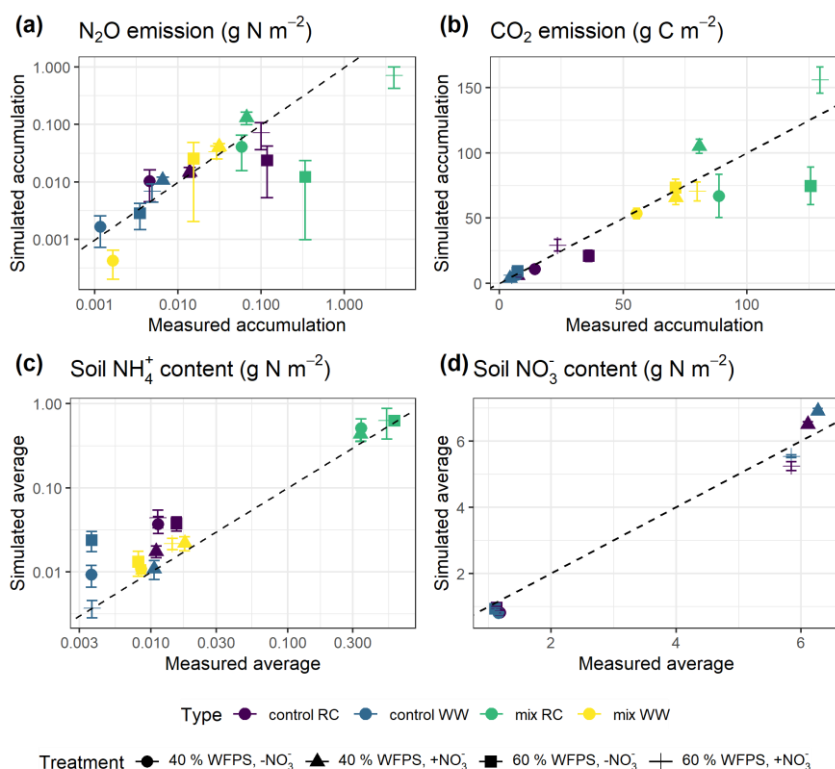
325

Figure 5: Simulated and measured daily N₂O fluxes (a), CO₂ fluxes (b), soil NH₄⁺ content (c), and soil NO₃⁻ content (d) during the 43-day incubation. Scatter points represent measured data; and triangles with dashed lines represent simulated data (error bar: 95 % confidence interval). Daily measurements presented were re-calculated from the data provided by Taghizadeh-Toosi et al. (2021).



3.2.2 Cumulative gas fluxes and average mineral N content

330 Model predictions of cumulative N_2O fluxes and CO_2 fluxes for the 16 treatments were significant and strongly correlated
 with the observed fluxes (Fig. 6 and Table 1). For N_2O , there was a bias towards underestimation of high cumulative N_2O
 fluxes (slope bias $\beta_1 = 0.17$, ME = -0.23). Estimate of slope in linear regression for cumulative CO_2 flux approached $\beta_1 = 1$
 indicating there was no consistent bias. For the average NH_4^+ and NO_3^- content, the estimated slopes were close to unity, and
 the deviations between prediction and measurement, signified by the relative RMSEs (rRMSEs), were 46 and 11 %,
 335 respectively. For the average NH_4^+ content in the low range, simulated values were found to overestimate the measured data
 (Fig. 6c).



340 **Figure 6: Simulated and measured cumulative N_2O fluxes (a), CO_2 fluxes (b), average NH_4^+ content (c), and average soil NO_3^- content (d) during the 43-day incubation (error bar: 95 % confidence interval). Reference lines with a slope of 1.0 are shown on the graphs.**

Table 1: Model evaluation of cumulative gas fluxes and average mineral N content from single-treatment calibration procedure and multi-treatment calibration procedure. The mean values of posterior models were compared with the observed data for 16 treatments. Units are valid for the statistics of ME and RMSE.



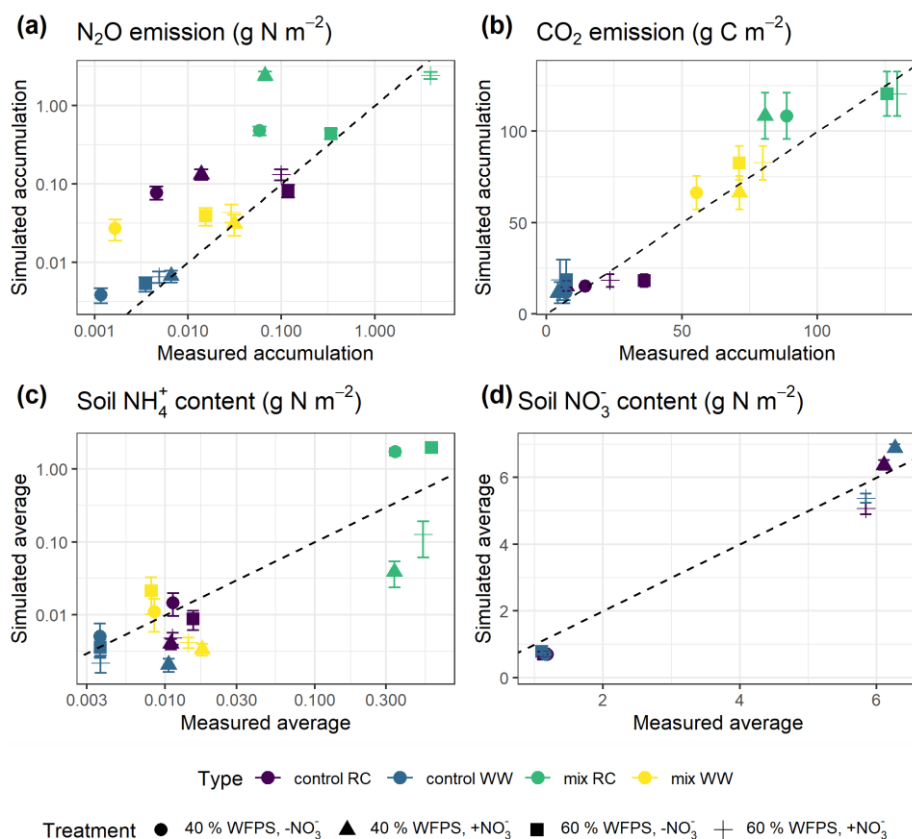
Calibration	Cumulative N ₂ O emission (g N m ⁻²)		Cumulative CO ₂ emission (g C m ⁻²)		Average NH ₄ ⁺ content (g N m ⁻²)		Average NO ₃ ⁻ content (g N m ⁻²)	
	Single- treatment	Multi- treatment	Single- treatment	Multi- treatment	Single- treatment	Multi- treatment	Single- treatment	Multi- treatment
ME	-0.23	0.10	-3.07	4.66	0.03	0.12	-0.11	-1.10
RMSE	0.82	0.71	17.2	12.1	0.06	0.50	0.41	0.50
rRMSE	275 %	238 %	34 %	24 %	46 %	411 %	11 %	14 %
Slope, β_1	0.17	0.56	0.93 ^a	0.97 ^a	1.15	2.13 ^a	1.07 ^a	1.08 ^a
Intercept, β_0	0.02	0.23	0.64	6.16	0.01	-0.01	-0.36	-0.53
R ²	0.96	0.47	0.84	0.93	0.98	0.50	0.98	0.98

345 ^a Values are not significantly different from one by one-sample *t*-tests (significance level $\alpha = 0.05$).

A regression of simulated cumulative N₂O flux residuals against observed data confirmed that underestimations were strongly ($R^2 = 0.92$) associated with the magnitude of observed N₂O fluxes (Fig. S1a). The negative slope of the regression indicated an underestimate of 0.83 g N₂O-N for every 1 g of observed N₂O-N per square meter. A regression of simulated cumulative N₂O flux residual against the residuals of other variables revealed that underestimations were not strongly associated with the residuals of simulated NH₄⁺ and NO₃⁻ (Fig. S1c and d). However, we observed that clustering of residuals concerning mineral N existed in which underestimations of cumulative N₂O flux tended to occur when soil NH₄⁺ was overestimated and when soil NO₃⁻ was underestimated. Specifically, residuals for cumulative N₂O flux and soil NO₃⁻ were simultaneously underestimated in 53 % of the posterior runs as revealed by scatter points falling in the third quadrant; and underestimations of N₂O flux were accompanied by overestimations of soil NH₄⁺ in 41 % of the posterior runs by looking at scattering points in the fourth quadrant. When only the subset of control treatments was analyzed, the clustering patterns became even more apparent (Fig. S2c and d).

3.2.3 Calibration by multiple treatments

Increasing the number of calibration treatments led to reduced uncertainty but, meanwhile, poor performances of posterior models for some treatments (Fig. 7). Cumulative N₂O fluxes were better simulated for the treatments with higher observed fluxes in each group, especially treatments at 60 % WFPS, but were overestimated for others with low observed fluxes. The regression between the mean simulated and measured N₂O flux only accounted for 47 % of the variation in the data, much lower than the level of 96 % in the single-treatment calibration procedure (Table 1). Simulated CO₂ and NO₃⁻ were generally close to the observed data. In the same group, simulated CO₂ fluxes were not different between two levels of NO₃⁻ input but depended on the level of moisture. Simulated soil NH₄⁺ showed a good agreement with the measured data in the low range of NH₄⁺ content, but had large model deviations for the four RC residue treatments, in which the R² was 0.50 in contrast to 0.98 in the single-treatment calibration procedure (Table 1).



370 **Figure 7: Simulated and measured cumulative N₂O fluxes (a), CO₂ fluxes (b), average NH₄⁺ content (c), and average soil NO₃⁻ content (d) during the 43-day incubation (error bar: 95 % confidence interval). Simulated results were obtained from multi-treatment calibration. Reference lines with a slope of 1.0 are shown on the graphs.**

3.2.4 Simulated oxygen status and N₂O sources

Simulated oxygen content in the soil cores was close to that of the ambient air, with the modeled volumetric oxygen content ranging from 19.5 % to 20 % throughout the incubation period for all treatments (Table S7). Still, according to the model, denitrification-derived N₂O accounted for 76-100 % of the total emissions on average (Table S7).

375 In simulations, the 0-4 cm soil layer was treated as one uniform compartment, and this could have influenced model predictions. To investigate whether increasing the vertical resolution could improve the model performance, the soil profile was uniformly divided into five layers. The results showed that underestimations of high N₂O fluxes still existed after this change in the vertical representation of the model (Table S6). The simulated soil oxygen profiles were still predominantly aerobic for all treatments, as the single-layer model, but showed stratification over depth as depicted in Fig. 8. The oxygen
380 level was the lowest at the beginning of incubation and then showed an increase over the period studied, mirroring the trends



of CO₂ flux. Despite the overall aerobic conditions in the soil, the large proportion of denitrification-derived N₂O emissions was accompanied by the rapid growth of denitrifier biomass (data not shown).

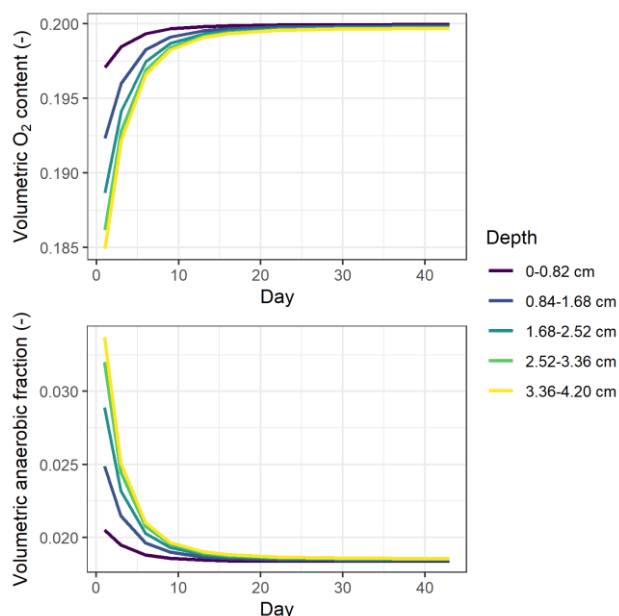


Figure 8: Simulated O₂ content and volumetric anaerobic fraction by the multi-layer model for the treatment with the greatest soil respiration rate (i.e. RC treatment with NO₃⁻ addition at 60 % WFPS). The mean daily values from posterior runs were used here.

385

3.2.5 Calibrated parameters

Although the number of parameters used for calibration had been reduced by Morris screening, more than half of the 26 calibrated parameters still exhibited random distributions within the predefined ranges (Fig. S4). The many potential inter-correlations may be the reason that these parameters could not be constrained to an unambiguous solution. But five parameters were showing marked variability in their posterior distributions between treatments as depicted in Fig. 9, where the prior ranges of these parameters are indicated in the ordinate.

390

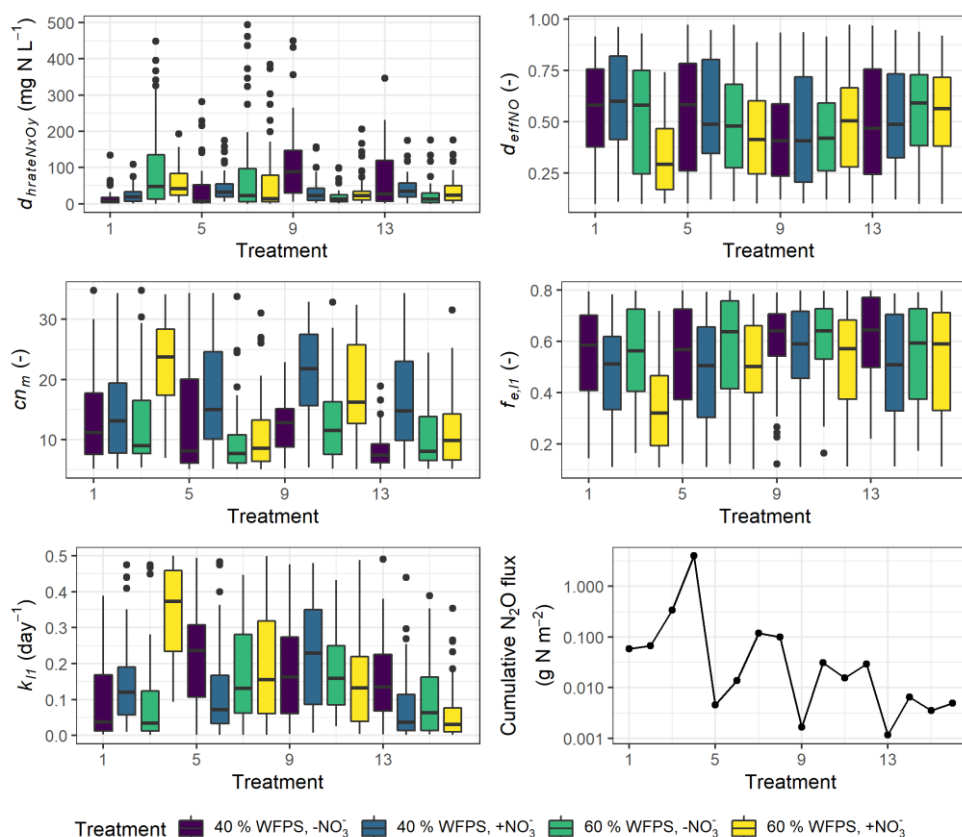
In most treatments, the parameter $d_{hrateN_xO_y}$ representing the N concentration for half rate in the denitrification process and also known as the Michaelis constant of the enzyme, was well constrained at the lower range of the parameter boundary within 50 mg N L⁻¹ in contrast to the mean of 250 mg N L⁻¹ in the prior range. A low $d_{hrateN_xO_y}$ relative to the physical concentration of NO₃⁻ resulted in a pronounced response of denitrifying bacteria activity to substrate availability (see Eq. (6.44) in Table S2). In some treatments which had no NO₃⁻ addition, i.e. treatment 3, 7, 9, and 13, the parameter showed more diffused distribution and higher medians compared to other treatments. An enzyme with high $d_{hrateN_xO_y}$ relative to the concentration of substrate is not normally saturated with substrate and thus the rate of formation of product is substrate-limited.

395



400 In more than half of the treatments, the posterior distribution of cn_m , the microbial C/N ratio (cn_m) involved in calculations of mineralization and immobilization, was concentrated around 10 on average. However, for some NO_3^- amended treatments which usually had higher N_2O emission rates, i.e. treatments 4, 6, 10, 12, and 14, the distribution of calibrated microbial C/N ratio was not well constrained but similar to the prior distribution with medians up to 20.

405 The parameter representing the rate coefficient for the decay of the litter carbon pool, k_{ll} generally showed higher values in WW treatments than controls, and its range for the high nitrate RC treatment at 60% WFPS (treatment 4) was markedly higher than other treatments, indicating the faster decomposition of labile organic matter. Besides, the efficiency of NO -based denitrifier respiration, d_{effNO} , showed a low-range distribution for treatment 4. Low d_{effNO} values induced a high respiration rate of denitrifiers for carrying out NO reduction (see Eq. (6.47) in Table S2). This treatment also exhibited a low-range distribution of the efficiency of SOM decomposition, $f_{e,ll}$, associated with a high fraction of CO_2 production.



410

Figure 9: Variability in five calibrated parameters among the 16 treatments. The boxplots show the 25 % and 75 % percentiles as the tops and bottoms of the boxes, and the medians as the bold lines. Treatment indices 1-4 represent treatments of mix RC, 5-8 for control RC, 9-12 for mix WW, and 13-16 for control WW, where treatment conditions are, in order: “40% WFPS, NO_3^- ”, “40% WFPS, $+\text{NO}_3^-$ ”, “60% WFPS, NO_3^- ”, and “60% WFPS, $+\text{NO}_3^-$ ”.



415 4 Discussion

4.1 Sensitivity analysis

The sensitivity analyses, investigating the impact of parameter uncertainties on model predictions, revealed the importance of parameter interactions and connections between different processes in the model (Fig. 3a-f). Compared with CO₂ emissions and soil NH₄⁺ content, N₂O emissions were controlled by a larger number of parameters related to decomposition and denitrification processes and had generally lower SEEs. According to Fig. 3a, the sizes of humus and litter pools and their decomposition rates were critical in reducing the uncertainty of simulating N₂O emissions. These results highlight the importance of reliable information on the initial state of the soil with respect to the composition and recalcitrance of organic matter pools where part of the organic matter within the soil cores could be fresh input from residues. The results confirm the findings of previous experimental and modeling studies showing the importance of substrate heterogeneity for decomposition and denitrification processes (Brilli et al., 2017; Eusterhues et al., 2003; Sierra et al., 2011). However, some other studies (Dungait et al., 2012; Schmidt et al., 2011) indicate that the chemical structure of organic molecules alone may not control their stability in soil, instead environmental and biological controls (e.g. accessibility of the SOM to decomposers, abiotic reactions, and desorption) predominate the SOM turnover especially in the longer term.

In our model simulations, C and N in crop residues were allocated to two labile pools, but the allocation ratio did not greatly influence N₂O emissions, soil respiration, or mineral N. This could be related to the fact that the overall C/N ratio of crop residues was kept constant as the sizes of organic matter pools changed in the sensitivity analysis. The influence of crop residues on N₂O emissions may be better reflected in other residue properties, e.g., the C/N ratio and solubility of individual substrates (Aulakh et al., 1991; Surey et al., 2020). Furthermore, it should be noted that addition of labile carbon from crop residues does not affect the decomposition of native soil organic matter in the model (i.e., no priming effect), as the decomposition of organic matter in labile and recalcitrant pools are calculated separately in CoupModel, similar as in other process-based models. The omission of a priming effect, the importance of which has been shown in field and laboratory studies (Kuzyakov, 2010), may cause models to underestimate the effects of crop residue composition on the turnover of soil C and N.

On the other hand, denitrifier growth parameters (e.g. d_{effNO} , $d_{growthNO3}$) showed considerable influence on the release of N₂O in most treatments (Fig. 3a). Our results suggested that the influences of microbial activities on N₂O emissions varied between different denitrification steps, and the denitrifier respiration for NO reduction showed a relatively larger and broader impact across treatments than other steps. The analysis of the two statistical measures σ and μ suggested that, rather than a single factor driving the model to become more ‘behavioral’ in predicting N₂O emissions, the collective effects of multiple parameters were more important, because one single parameter could exhibit various SEEs as other parameters changed, represented by high variability (σ) compared to the mean (μ) in Fig. 3d. In calibrating complex models, several combinations of different parameter values might give the same goodness-of-fit between model outputs and measured variables, which is



450 defined as equifinality (Beven and Freer, 2001). The model sensitivity to such parameters is probably attenuated in the case of high-level equifinalities. Besides, the importance of parameter interaction structure associated with equifinality could hinder the constraint of parameters and hence the reduction of uncertainty in N₂O simulations when limited measurement data are available. For instance, the fraction of C mineralized to CO₂, characterized by (1- $f_{e,11}$), and the decay rate of litter1 (k_{l1}), have a product interaction regarding the production of CO₂ (see Eq. (6.3) and Eq. (6.4) in Table S2). Also, the denitrifier growth rates (e.g. $d_{growthNO_3}$) and the Michaelis constant characterized by $d_{hrateN_xO_y}$ influence the loss of N from anaerobic N pools by invoking microbial growth via a quotient interaction (see Eq. (6.41) and Eq. (6.44) in Table S2).

455 The parameters found to have the greatest impact on soil respiration and NH₄⁺ content were associated with SOM composition (SOC_h) and decomposability (k_{l1} , k_{l2} , $f_{e,11}$, $f_{e,12}$), suggesting that model uncertainty for soil respiration and soil NH₄⁺ could be greatly reduced if data for either SOM composition or decay rates were available. For simulating soil NH₄⁺, information about microbial C/N ratio (cn_m) and denitrifier growth parameters (e.g. $d_{growthNO_3}$) is also important, because the availability of soil mineral N is closely associated with decomposition dynamics and its consumption by immobilization, nitrification, and denitrification (Lashermes et al., 2022). The influences of soil porosity and wilting point on CO₂ emissions and soil NH₄⁺ content were larger under, respectively, wet and dry conditions. The results can be explained by the fact that 460 soil porosity and wilting point are key set points of the soil moisture response function controlling the upper and lower bounds of the function, which implies that the measurement of soil hydraulic properties could reduce model uncertainty under contrasting soil moisture levels.

4.2 Model performance and possible explanations for deviations

465 Overall, the performance of posterior models varied between estimated variables and treatments. The timing and magnitude of peak N₂O emissions were more difficult to predict than those of CO₂ emissions even though parameters had been adjusted for individual treatments, and negative errors relative to observations were seen particularly when simulating high N₂O emissions. Evaluation of model bias with respect to the slope β_1 in linear regression demonstrated a tendency across treatments to increasingly underestimate cumulative N₂O flux as the observed flux increased. The problem of 470 underestimating high N₂O fluxes by process-oriented models has been reported in previous studies. For example, Fang et al. (2015) showed that four different algorithms all underestimated the four highest cumulative N₂O fluxes among eight N fertilizer treatments in an irrigated cornfield. Also, Gaillard et al. (2018) evaluated the simulated N₂O flux from three process-oriented models (DNDC, DayCent, and EPIC) and reported an underestimation of 0.01-0.93 kg N₂O-N ha⁻¹ for every 1 kg of observed N₂O-N ha⁻¹ across models.

475 Residual analysis revealed that the model had a tendency to simultaneously underestimate NO₃⁻ and overestimate NH₄⁺ when N₂O emission was underestimated, and this trend was even more pronounced when looking at control treatments only (Figs. S1 and S2). This suggests the nitrification rates may have been underestimated by the model and calls for revisiting the parameterization of the nitrification process. The simulated accumulation of NH₄⁺ in the RC residue treatments, in contrast to



480 the transient NH_4^+ peaks observed (Fig. 5c), indicates that the modeled NH_4^+ release linked to decomposition was greater than the NH_4^+ consumption by microbial immobilization and nitrification simulated. Nylander et al. (2011) showed that a low nitrification rate simulated by the CoupModel was possibly the reason for the overestimation of the amount of soil NH_4^+ in a model of an organic cropping system. In our study, however, the weak and insignificant relationship between N_2O flux residuals and the residuals for mineral N indicates that N_2O underestimation at high flux ranges may be due to other factors.

485 Inaccurate estimation of proximal factors such as soil water content and temperature by the pedo-climatic subroutines has been a main cause of errors in simulating C and N emissions in many process-based models (Brilli et al., 2017). In our study, the soil water content and temperature were assumed constant during incubation, but heterogeneity in the distribution of water could be a problem when initializing the soil environment in the model. Water retention capacity in the soil might be altered by the practice of adding crop residues. Lashermes et al. (2021) found that adding crop residues to soil increased the average WFPS of this layer from 60 % to 63 %. Kravchenko et al. (2017) found that specific gravimetric moisture of plant
490 residues in soil could vary in the range 60-220 %, and that residues were characterized by high moisture even at low soil water contents. Hence, the main effect of crop residues on the abiotic soil environment is probably not the marginal change in the average soil moisture content, but more likely the co-occurrence of elevated water content and labile C and N within the soil core. Residue fragments with high water retention capacity could represent microenvironments markedly different from those of the bulk soil and promote N_2O emissions (Kravchenko et al., 2017). Model results indicated that the simulated
495 O_2 content at 0-4 cm depth had only slight changes overall during incubation and was close to the saturation partial pressure in soil air owing to faster diffusion supply compared to soil respiration rates (Fig. 8). In the experiments, most of the oxygen consumption likely occurred in the microenvironment around residue debris. This is supported by observations of O_2 concentration in soil using O_2 microsensors (Markfoged et al., 2011) and planar optodes (Kravchenko et al., 2017) showing the aerated O_2 partial pressure in the soil matrix away from organic hotspots and steep gradients in O_2 between bulk soil and hotspots of manure and residues, respectively. Nevertheless, simulations showed that denitrification was the major N_2O
500 producing process in the experiment, accounting for 76-100 % of the total estimated N_2O emissions. Parkin (1987) found that a thin water film even as little as 20 μm , could be enough to deplete air and support denitrification at the surface of decaying litter, and it is thus possible that the observed high N_2O fluxes were produced via denitrification despite an overall high aeration status within the soil. Water absorption by residue fragments from the surrounding soil could create local
505 anoxic environments conducive to denitrification while also enabling the release of produced gases via drained pores (Kravchenko et al., 2018). In existing process-based models the heterogeneity in physical and biochemical processes caused by organic amendments is not included, which may limit the ability of these models to reflect the microscale anaerobiosis and SOC availability, and to predict peak N_2O emissions such as those observed in RC treatments (Fig. 5a). Some studies explored possibilities to incorporate spatial variability into denitrification models, although conceptual frameworks
510 considering heterogeneous environments for greenhouse gas emissions have only in recent years emerged and gained attention (Sihi et al., 2020). Using a stochastic modeling approach, Parkin (1987) found that the patchy dispersion pattern of



515 high denitrification microsites was a major factor influencing the overall rates of denitrification. Based on a parsimonious numerical model, Sihi et al. (2020) used probability distribution functions to represent soil microsite production and consumption of three greenhouse gases, which explained occasional observations of simultaneous N₂O uptake (reduction) and CH₄ uptake (oxidation) that were not typically captured by other models. We suggest that model development should improve on the description of microscale processes in soil, for example by parameterizing the distribution and extent of heterogeneity in, e.g., organic amendments and clay content, and by establishing the degree of anaerobiosis associated with hotspots and bulk soil separately.

520 The simultaneous underestimation of N₂O and NO₃⁻ could be linked to the incomplete description of nitrate supply in the residue-amended 0-4 cm soil layer, which assumed there was no exchange with the lower 4-8 cm bulk soil layer. In a separate incubation experiment using the same soil type and several of the same treatments, Lashermes et al. (2021) found that adding RC residue to the 0-4 cm soil layer induced a decrease in the NO₃⁻ content of the unamended 4-8 cm depth layer, indicating that the above, amended layer influenced the NO₃⁻ dynamics in the bottom layer presumably caused by mass transfer between the two layers due to net consumption of NO₃⁻ within the top layer during denitrification. In the current model framework, solute transport is only simulated by convection (driven by water flow) and does not include diffusion driven by concentration gradients. The model was originally designed for field conditions, and at this spatial scale infiltration is the main mechanism for solute transport between compartments. However, in the short term after organic amendments, diffusive NO₃⁻ supply from the bulk soil can be the most important source of electron acceptor for denitrification, as observed in earlier incubation studies (Nielsen et al., 1996; Petersen et al., 1996). The current solute transport process may thus not be sufficient to properly simulate N₂O production in microbial hotspots, especially under low flow rates or for short travel distances where diffusive flux becomes increasingly important (Flury and Gimmi, 2002). Microbial turnover could accelerate the recycling of N and increase substrate availability for nitrification and denitrification locally (De Bruijn et al., 2009), but in this and some other process-based models, microbial N is not connected to the mineral N pool or included in the calculation of total N budget, which could be another reason for model discrepancies in mineral N dynamics.

535 Only a few parameters showed distinct probability distribution patterns after calibration while others exhibited uniform distributions as the prior sampling. This result was in accordance with the second hypothesis, which should be related to the limited size of calibration data set in each treatment and the equifinalities between parameters. The differences in the posterior parameter distribution hold information about the characteristics of simulated C and N processes between treatments, although such variability may also reflect potential model limitations. For example, the well-constrained microbial biomass C/N ratio (cn_m) within 10 in most treatments was consistent with observations that, on average, the C/N ratio of the soil microbial biomass varies between 6 and 10 at a global scale (Xu et al., 2013) and does not easily adapt in composition to litter quality (Spohn, 2015). Fungal cells typically have a C/N ratio ranging from 10 to 15 while bacteria range from 3.5 to 7 (Paul, 2007). In some treatments associated with extra NO₃⁻ input and high N₂O emissions, the microbial C/N ratios in accepted runs exhibited relatively high values, closer to the soil-residue mixture C/N ratio. According to Eq.



545 (6.7) and Eq. (6.8) in Table S2, a relatively high cn_m could lead to a low level of humification (i.e. less labile C and N
converted to recalcitrant matter) as well as intense N mineralization (i.e. more organic N in litter pools converted to NH_4^+).
This could be associated with the underestimation of NO_3^- availability discussed above, especially for the treatments
amended with crop residues. Meanwhile, the relatively low values of estimated Michaelis constant $d_{hrateN_xO_y}$ suggested a high
550 microbial affinity for soluble nitrogen oxides, accelerating microbial denitrification. In treatments without NO_3^- addition,
respiration via denitrification could be limited by the availability of electron acceptors through the respiratory chain,
explaining an increase in the apparent Michaelis constant for N substrate reduction (Khalil et al., 2005). Including solute
diffusion in the model may be able to change the posterior distributions of both parameters by better mimicking the mineral
N supply. Compared to control treatments, the faster decay of organic matter (k_{11} , k_{12}) and higher CO_2 formation rate ($f_{e,11}$,
 $f_{e,12}$) in the crop residue treatments could reflect the need to mobilize N for use in nitrification and denitrification processes.
555 Fast organic matter turnover in the residue-soil mixture was possibly caused by a high concentration of decomposer
microorganisms associated with residue fragments. Additionally, in contrast to natural soils, human disturbance of the soil in
the laboratory could stimulate indigenous microbial communities resulting in rapid biological phenomena (Calderon et al.,
2001; Thiessen et al., 2013).

It should be noted that the model deviations for N_2O flux were not caused by the spatial resolution of the vertical soil profile,
560 which has been a problem in some studies (e.g. Xing et al., 2011), as the model performance concerning N_2O prediction was
not improved in the multi-layer model (Table S6) where the one-layer soil profile had been sub-divided into five layers for
simulations. Deviations between modeled results and measured values are more likely to have resulted from limitations in
the description of the N processes behind N_2O emissions. For example, increasing the number of layers would not reflect the
microscale processes associated with crop residue fragments and soil aggregates, nor would it address the missing
565 description of solute diffusion between interfaces.

4.3 Treatment effects

We did not investigate how the model responded to the specific change of soil moisture and NO_3^- level, but the results we
obtained after calibrating the model against multiple treatments indicated the challenges in predicting N_2O emissions under
varying soil environmental conditions using a common model parameterization (Fig. 7). Similar cumulative N_2O fluxes were
570 simulated for treatments with the same NO_3^- level regardless of the soil moisture level, which was different from
observations. In the experiment, in RC treatments higher N_2O fluxes were associated with the higher WFPS level (60 %)
rather than with the higher NO_3^- level, although there was a strong interaction between the two factors (Taghizadeh-Toosi et
al., 2021). The problem to describe treatment effects of incubation studies by process-based models was discussed in a recent
study by Grosz et al. (2021) who found that three N_2O models (DNDC, CoupModel, and DeNi) responded to controlling
575 factors in the same direction as measurements with frequencies from only 19 % to 67 %. Different from their study, in which
no systematic calibration of model parameters was performed, the model deviations in our study, obtained by calibration of



multiple treatments, suggested that potential limitations in model assumptions or the description of mechanisms were more critical reasons for unsatisfactory model responses than parameterization. In CoupModel, while the denitrification subroutine is sensitive to changes in soil temperature, pH, mineral N, and SOC content, the soil moisture has indirect and average effects on denitrification through decomposition, nitrification, and gas diffusion processes, but the effects of heterogeneity in the distribution of water and microbial activities are not represented. Therefore, soil moisture may have less effect on the N₂O flux estimation in model applications than in real soil environments with heterogeneity in the distribution of C and N sources, and moisture. This is still one of the most challenging tasks facing soil biogeochemical models. On the other hand, our results showed a tendency to better predict treatments with higher N₂O fluxes in the same group. This can be understood from the characteristics of the calibration dataset and selection criteria. The high flux samples represented only a minor fraction of the total samples (i.e. 40 sampling points) in each group but were higher than the rest of them by orders of magnitude (Fig. 5a). The application of the ME criterion mainly constrained model deviations for the high fluxes in one data set, and less so for minor fluxes. It may be argued that this limitation could be improved by applying more stringent additional criteria such as R². However, this would reduce the acceptance rate or even refuse all posterior runs. Interestingly, Vezzaro et al. (2012) obtained similar results in a GLUE context by using the Nash-Sutcliffe-based likelihood and stormwater measurements with large internal variability, and concluded that the choice of selection criteria should be based not only on its mathematical features but also by looking at the characteristics of the available data.

We also found that our capacity to evaluate model performance was limited by the data available for model estimation and calibration. Some model parameters were not assessed in the incubation experiment (e.g. soil/residue labile C content and microbial biomass) and their values were either estimated or determined by calibration. The quality and temporal resolution in the measurement of controlling factors such as NO₃⁻ and NH₄⁺ were limited, and improving these aspects may reduce uncertainty in model prediction and facilitate model evaluation. By looking at the patterns of simulated N₂O emissions and ancillary variables, we identified potential problems behind model principles, which should be investigated with experimental studies designed carefully for model use. Previous studies, including global sensitivity analyses (Metzger et al., 2016; Wu et al., 2019) and model evaluations (Grosz et al., 2021), have specific suggestions to this end, such as improving measurement frequencies, evaluating sensitive input variables (e.g. decomposability of labile C), measuring more variables regarding N cycle (e.g. N₂, NO) and using state-of-the-art techniques (e.g. ¹⁵N gas flux methods). We understand that collecting all data types discussed here is not always possible or practical, but encourage modelers to report more model outputs regarding N cycles even in the absence of observations, particularly the denitrification products, soil oxygen content, and anaerobic fraction, which was not done very often in previous studies.

5 Conclusion

The current setup of CoupModel, when applied to results from an incubation study, indicated that parameters associated with the decomposability of SOM and denitrifier growth were important in regulating soil respiration and mineral N dynamics. A



610 high level of parameter interaction and equifinality issues existed regarding N₂O emissions, hindering the determination of sensitivities and parameter constraints.

The parameters showing posterior distributions that differed from the prior distributions revealed specific modeled microbial processes between treatments and may be used as references behind observations. For example, in the treatments without NO₃⁻ addition, the availability of N substrates to denitrifiers was limited according to the posterior distribution of Michaelis constants. More intense SOM decomposition was simulated in residue treatments compared to controls.

615 The uncertainty analysis demonstrated a model bias towards underestimating high-range daily and cumulative N₂O fluxes, which was associated with an inaccurate description of mineral N dynamics. Residual analysis indicated that nitrification rate could be underestimated but did not sufficiently explain the model deviations. While the simulated soil respiration response to soil moisture was generally in line with the direction of measurement, the modeled N₂O emissions were not as sensitive to the WFPS as the measured data, probably because of the indirect effect of soil moisture response function on the denitrification process. Discussing potential limitations in model principles related to the prediction bias, we described several suggestions for model improvement including the use of new parameters and equations to represent microscale heterogeneity, and a re-examination of the effects of soil moisture on denitrification processes.

620 Generally, we conclude that modeling N₂O emissions in controlled experiments is useful to identify the need for prior knowledge in both basic (e.g. decomposability of SOM) and elaborate (e.g. denitrifier growth) aspects of the process-based model for reducing the uncertainty of N₂O flux estimates. Moreover, we identified a potential model bias and discussed future steps that may be required to assess its sources. We believe there is a need to modify model equations and revisit basic model assumptions with high-quality measurement data sets that enable more intensive model evaluations and comparisons.

Acknowledgments

630 This study was financially supported by Independent Research Fund Denmark (DRF) (Project acronym: modelN2O). Dr. Arezoo Taghizadeh-Toosi is acknowledged for having provided the experimental data. We further thank Iris Vogeler Cronin for providing insights on the model results. Zhang W. acknowledged grant from the Swedish Research Council VR 2020-05338.



References

- 635 Abdalla, M., Jones, M., Yeluripati, J., Smith, P., Burke, J. and Williams, M.: Testing DayCent and DNDC model simulations of N₂O fluxes and assessing the impacts of climate change on the gas flux and biomass production from a humid pasture, *Atmos. Environ.*, 44, 2961–2970, doi:10.1016/j.atmosenv.2010.05.018, 2010.
- Aulakh, M. S., Walters, D. T., Doran, J. W., Francis, D. D. and Mosier, A. R.: Crop residue type and placement effects on denitrification and mineralization, *Soil Sci. Soc. Am. J.*, 55, 1020–1025, doi:10.2136/SSSAJ1991.03615995005500040022X, 1991.
- 640 Beven, K. and Binley, A.: The future of distributed models: model calibration and uncertainty prediction, *Hydrol. Process.*, 6, 279–298, doi:10.1002/HYP.3360060305, 1992.
- Beven, K. and Freer, J.: Equifinality, data assimilation, and uncertainty estimation in mechanistic modelling of complex environmental systems using the GLUE methodology, *J. Hydrol.*, 249, 11–29, doi:10.1016/S0022-1694(01)00421-8, 2001.
- 645 Brilli, L., Bechini, L., Bindi, M., Carozzi, M., Cavalli, D., Conant, R., Dorich, C. D., Doro, L., Ehrhardt, F., Farina, R., Ferrise, R., Fitton, N., Francaviglia, R., Grace, P., Iocola, I., Klumpp, K., Léonard, J., Martin, R., Massad, R. S., Recous, S., Seddaiu, G., Sharp, J., Smith, P., Smith, W. N., Soussana, J.-F. and Bellocchi, G.: Review and analysis of strengths and weaknesses of agro-ecosystem models for simulating C and N fluxes, *Sci. Total Environ.*, 598, 445–470, doi:10.1016/j.scitotenv.2017.03.208, 2017.
- De Bruijn, A. M. G., Butterbach-Bahl, K., Blagodatsky, S. and Grote, R.: Model evaluation of different mechanisms driving 650 freeze–thaw N₂O emissions, *Agric. Ecosyst. Environ.*, 133, 196–207, doi:10.1016/j.agee.2009.04.023, 2009.
- Chen, D., Li, Y., Grace, P. and Mosier, A. R.: N₂O emissions from agricultural lands: a synthesis of simulation approaches, *Plant Soil*, 309, 169–189, doi:10.1007/s11104-008-9634-0, 2008.
- Davidson, E. A. and Kanter, D.: Inventories and scenarios of nitrous oxide emissions, *Environ. Res. Lett.*, 9, 105012, doi:10.1088/1748-9326/9/10/105012, 2014.
- 655 Dungait, J. A. J., Hopkins, D. W., Gregory, A. S. and Whitmore, A. P.: Soil organic matter turnover is governed by accessibility not recalcitrance, *Glob. Chang. Biol.*, 18, 1781–1796, doi:10.1111/j.1365-2486.2012.02665.x, 2012.
- Eusterhues, K., Rumpel, C., Kleber, M. and Kögel-Knabner, I.: Stabilisation of soil organic matter by interactions with minerals as revealed by mineral dissolution and oxidative degradation, *Org. Geochem.*, 34, 1591–1600, doi:10.1016/j.orggeochem.2003.08.007, 2003.
- 660 Fang, Q. X., Ma, L., Halvorson, A. D., Malone, R. W., Ahuja, L. R., Del Grosso, S. J. and Hatfield, J. L.: Evaluating four nitrous oxide emission algorithms in response to N rate on an irrigated corn field, *Environ. Model. Softw.*, 72, 56–70,



doi:10.1016/j.envsoft.2015.06.005, 2015.

Firestone, M. K. and Davidson, E. A.: Microbiological basis of NO and N₂O production and consumption in soil, *Exch. Trace Gases between Terr. Ecosyst. Atmos.*, 47, 7–21, 1989.

665 Flury, M. and Gimmi, T. F.: 6.2 Solute Diffusion, in *Methods of Soil Analysis: Part 4 Physical Methods*, edited by J. H. Dane and C. G. Topp, pp. 1323–1351, Soil Science Society of America, Inc., Madison, U.S., 2002.

Gabrielle, B., Laville, P., Duval, O., Nicoullaud, B., Germon, J. C. and Hénault, C.: Process-based modeling of nitrous oxide emissions from wheat-cropped soils at the subregional scale, *Global Biogeochem. Cycles*, 20, GB4018, doi:10.1029/2006GB002686, 2006.

670 Gaillard, R. K., Jones, C. D., Ingraham, P., Collier, S., Izaurrealde, R. C., Jokela, W., Osterholz, W., Salas, W., Vadas, P. and Ruark, M. D.: Underestimation of N₂O emissions in a comparison of the DayCent, DNDC, and EPIC models, *Ecol. Appl.*, 28, 694–708, doi:10.1002/eap.1674, 2018.

675 Gijsman, A. J., Hoogenboom, G., Parton, W. J. and Kerridge, P. C.: Modifying DSSAT crop models for low-input agricultural systems using a soil organic matter–residue module from CENTURY, *Agron. J.*, 94, 462–474, doi:10.2134/agronj2002.4620, 2002.

Goreau, T. J., Kaplan, W. A., Wofsy, S. C., McElroy, M. B., Valois, F. W. and Watson, S. W.: Production of NO₂⁻ and N₂O by nitrifying bacteria at reduced concentrations of oxygen, *Appl. Environ. Microbiol.*, 40, 526–532, doi:10.1128/aem.40.3.526-532.1980, 1980.

680 Grandy, A. S. and Robertson, G. P.: Initial cultivation of a temperate-region soil immediately accelerates aggregate turnover and CO₂ and N₂O fluxes, *Glob. Chang. Biol.*, 12, 1507–1520, doi:10.1111/j.1365-2486.2006.01166.x, 2006.

Grosz, B., Well, R., Dechow, R., Köster, J. R., Khalil, M. I., Merl, S., Rode, A., Ziehmer, B., Matson, A. and He, H.: Evaluation of denitrification and decomposition from three biogeochemical models using laboratory measurements of N₂, N₂O and CO₂, *Biogeosciences*, 18, 5681–5697, doi:10.5194/bg-18-5681-2021, 2021.

685 Jansson, P.-E.: CoupModel: model use, calibration, and validation, *Trans. ASABE*, 55, 1335–1344, doi:10.13031/2013.42245, 2012.

Jansson, P.-E. and Karlberg, L.: Coupled heat and mass transfer model for soil-plant-atmosphere systems, [online] Available from: <https://www.coupmodel.com/documentation> (Accessed 10 February 2022), 2010.

Jansson, P.-E. and Moon, D. S.: A coupled model of water, heat and mass transfer using object orientation to improve flexibility and functionality, *Environ. Model. Softw.*, 16, 37–46, doi:10.1016/S1364-8152(00)00062-1, 2001.



- 690 Keating, B. ., Carberry, P. ., Hammer, G. ., Probert, M. ., Robertson, M. ., Holzworth, D., Huth, N. ., Hargreaves, J. N. ., Meinke, H., Hochman, Z., McLean, G., Verburg, K., Snow, V., Dimes, J. ., Silburn, M., Wang, E., Brown, S., Bristow, K. ., Asseng, S., Chapman, S., McCown, R. ., Freebairn, D. . and Smith, C. .: An overview of APSIM, a model designed for farming systems simulation, *Eur. J. Agron.*, 18, 267–288, doi:10.1016/S1161-0301(02)00108-9, 2003.
- Khalil, K., Renault, P., Guerin, N. and Mary, B.: Modelling denitrification including the dynamics of denitrifiers and their progressive ability to reduce nitrous oxide: comparison with batch experiments, *Eur. J. Soil Sci.*, 56, 491–504, doi:10.1111/j.1365-2389.2004.00681.x, 2005.
- 695 Kravchenko, A. N., Toosi, E. R., Guber, A. K., Ostrom, N. E., Yu, J., Azeem, K., Rivers, M. L. and Robertson, G. P.: Hotspots of soil N₂O emission enhanced through water absorption by plant residue, *Nat. Geosci.*, 10, 496–500, doi:10.1038/ngeo2963, 2017.
- 700 Kravchenko, A. N., Fry, J. E. and Guber, A. K.: Water absorption capacity of soil-incorporated plant leaves can affect N₂O emissions and soil inorganic N concentrations, *Soil Biol. Biochem.*, 121, 113–119, doi:10.1016/J.SOILBIO.2018.03.013, 2018.
- Kuzyakov, Y.: Priming effects: interactions between living and dead organic matter, *Soil Biol. Biochem.*, 42, 1363–1371, doi:10.1016/j.soilbio.2010.04.003, 2010.
- 705 Kuzyakov, Y. and Blagodatskaya, E.: Microbial hotspots and hot moments in soil: concept & review, *Soil Biol. Biochem.*, 83, 184–199, doi:10.1016/j.soilbio.2015.01.025, 2015.
- Lashermes, G., Recous, S., Alavoine, G., Janz, B., Butterbach-Bahl, K., Ernfors, M. and Laville, P.: N₂O emissions from decomposing crop residues are strongly linked to their initial soluble fraction and early C mineralization, *Sci. Total Environ.*, 806, 150883, doi:10.1016/j.scitotenv.2021.150883, 2022.
- 710 Li, C., Frohling, S. and Frohling, T. A.: A model of nitrous oxide evolution from soil driven by rainfall events: 1. model structure and sensitivity, *J. Geophys. Res. Atmos.*, 97, 9759–9776, doi:10.1029/92JD00509, 1992.
- Li, C., Aber, J., Stange, F., Butterbach-Bahl, K. and Papen, H.: A process-oriented model of N₂O and NO emissions from forest soils: 1. model development, *J. Geophys. Res. Atmos.*, 105, 4369–4384, doi:10.1029/1999JD900949, 2000.
- Markfoged, R., Nielsen, L. P., Nyord, T., Ottosen, L. D. M. and Revsbech, N. P.: Transient N₂O accumulation and emission caused by O₂ depletion in soil after liquid manure injection, *Eur. J. Soil Sci.*, 62, 541–550, doi:10.1111/j.1365-2389.2010.01345.x, 2011.
- 715 Metzger, C., Nilsson, M. B., Peichl, M. and Jansson, P.-E.: Parameter interactions and sensitivity analysis for modelling carbon heat and water fluxes in a natural peatland, using CoupModel v5, *Geosci. Model Dev.*, 9, 4313–4338,



doi:10.5194/gmd-9-4313-2016, 2016.

- 720 Morris, M. D.: Factorial sampling plans for preliminary computational experiments, *Technometrics*, 33, 161–174, doi:10.1080/00401706.1991.10484804, 1991.
- Nielsen, T. H., Nielsen, L. P. and Revsbech, N. P.: Nitrification and coupled nitrification-denitrification associated with a soil-manure interface, *Soil Sci. Soc. Am. J.*, 60, 1829–1840, doi:10.2136/sssaj1996.03615995006000060031x, 1996.
- Norman, J., Jansson, P.-E., Farahbakhshazad, N., Butterbach-Bahl, K., Li, C. and Klemetsson, L.: Simulation of NO and N₂O emissions from a spruce forest during a freeze/thaw event using an N-flux submodel from the PnET-N-DNDC model integrated to CoupModel, *Ecol. Modell.*, 216, 18–30, doi:10.1016/j.ecolmodel.2008.04.012, 2008.
- 725 Nylinder, J., Stenberg, M., Jansson, P.-E., Klemetsson, Å. K., Weslien, P. and Klemetsson, L.: Modelling uncertainty for nitrate leaching and nitrous oxide emissions based on a Swedish field experiment with organic crop rotation, *Agric. Ecosyst. Environ.*, 141, 167–183, doi:10.1016/j.agee.2011.02.027, 2011.
- 730 Parkin, T. B.: Soil microsites as a source of denitrification variability, *Soil Sci. Soc. Am. J.*, 51, 1194–1199, doi:10.2136/sssaj1987.03615995005100050019x, 1987.
- Parton, W. J., Mosier, A. R., Ojima, D. S., Valentine, D. W., Schimel, D. S., Weier, K. and Kulmala, A. E.: Generalized model for N₂ and N₂O production from nitrification and denitrification, *Global Biogeochem. Cycles*, 10, 401–412, doi:10.1029/96GB01455, 1996.
- 735 Paul, E. A., Ed.: *Soil microbiology, ecology and biochemistry*, 3rd ed., Elsevier, Amsterdam, Netherlands., 2007.
- Petersen, S. O., Nielsen, T. H., Frostegård, Å. and Olesen, T.: O₂ uptake, C metabolism and denitrification associated with manure hot-spots, *Soil Biol. Biochem.*, 28, 341–349, doi:10.1016/0038-0717(95)00150-6, 1996.
- Ratto, M., Tarantola, S. and Saltelli, A.: Sensitivity analysis in model calibration: GSA-GLUE approach, *Comput. Phys. Commun.*, 136, 212–224, doi:10.1016/S0010-4655(01)00159-X, 2001.
- 740 Schmidt, M. W. I., Torn, M. S., Abiven, S., Dittmar, T., Guggenberger, G., Janssens, I. A., Kleber, M., Kögel-Knabner, I., Lehmann, J., Manning, D. A. C., Nannipieri, P., Rasse, D. P., Weiner, S. and Trumbore, S. E.: Persistence of soil organic matter as an ecosystem property, *Nature*, 478, 49–56, doi:10.1038/nature10386, 2011.
- Sierra, C. A., Harmon, M. E. and Perakis, S. S.: Decomposition of heterogeneous organic matter and its long-term stabilization in soils, *Ecol. Monogr.*, 81, 619–634, doi:10.1890/11-0811.1, 2011.
- 745 Sihi, D., Davidson, E. A., Savage, K. E. and Liang, D.: Simultaneous numerical representation of soil microsite production and consumption of carbon dioxide, methane, and nitrous oxide using probability distribution functions, *Glob. Chang. Biol.*,



26, 200–218, doi:10.1111/gcb.14855, 2020.

Sin, G., Gernaey, K. V. and Lantz, A. E.: Good modeling practice for PAT applications: propagation of input uncertainty and sensitivity analysis, *Biotechnol. Prog.*, 25, 1043–1053, doi:10.1021/bp.166, 2009.

750 Sommer, S. G., Petersen, S. O. and Møller, H. B.: Algorithms for calculating methane and nitrous oxide emissions from manure management, *Nutr. Cycl. Agroecosystems*, 69, 143–154, doi:10.1023/B:FRES.0000029678.25083.fa, 2004.

Spohn, M.: Microbial respiration per unit microbial biomass depends on litter layer carbon-to-nitrogen ratio, *Biogeosciences*, 12, 817–823, doi:10.5194/bg-12-817-2015, 2015.

755 Surey, R., Schimpf, C. M., Sauheitl, L., Mueller, C. W., Rummel, P. S., Dittert, K., Kaiser, K., Böttcher, J. and Mikutta, R.: Potential denitrification stimulated by water-soluble organic carbon from plant residues during initial decomposition, *Soil Biol. Biochem.*, 147, 107841, doi:10.1016/j.soilbio.2020.107841, 2020.

Syakila, A. and Kroeze, C.: The global nitrous oxide budget revisited, *Greenh. Gas Meas. Manag.*, 1, 17–26, doi:10.3763/ghgmm.2010.0007, 2011.

760 Taghizadeh-Toosi, A., Janz, B., Labouriau, R., Olesen, J. E., Butterbach-Bahl, K. and Petersen, S. O.: Nitrous oxide emissions from red clover and winter wheat residues depend on interacting effects of distribution, soil N availability and moisture level, *Plant Soil*, 466, 121–138, doi:10.1007/s11104-021-05030-8, 2021.

U.S. Environmental Protection Agency: Guidance on the development, evaluation, and application of environmental models (report no. EPA/100/K-09/003), [online] Available from: https://www.epa.gov/sites/default/files/2015-04/documents/cred_guidance_0309.pdf (Accessed 9 February 2022), 2009.

765 Uzoma, K. C., Smith, W., Grant, B., Desjardins, R. L., Gao, X., Hanis, K., Tenuta, M., Goglio, P. and Li, C.: Assessing the effects of agricultural management on nitrous oxide emissions using flux measurements and the DNDC model, *Agric. Ecosyst. Environ.*, 206, 71–83, doi:10.1016/j.agee.2015.03.014, 2015.

770 Vezzano, L. and Mikkelsen, P. S.: Application of global sensitivity analysis and uncertainty quantification in dynamic modelling of micropollutants in stormwater runoff, *Environ. Model. Softw.*, 27–28, 40–51, doi:10.1016/j.envsoft.2011.09.012, 2012.

Vezzano, L., Eriksson, E., Ledin, A. and Mikkelsen, P. S.: Quantification of uncertainty in modelled partitioning and removal of heavy metals (Cu, Zn) in a stormwater retention pond and a biofilter, *Water Res.*, 46, 6891–6903, doi:10.1016/j.watres.2011.08.047, 2012.

775 Wijler, J. and Delwiche, C. C.: Investigations on the denitrifying process in soil, *Plant Soil*, 5, 155–169, doi:10.1007/BF01343848, 1954.



World Meteorological Organization: WMO Greenhouse gas bulletin: the state of greenhouse gases in the atmosphere based on global observations through 2020, [online] Available from:

https://library.wmo.int/index.php?lvl=notice_display&id=21975#.YgFFTrrMJaq (Accessed 7 February 2022), 2021.

780 Wu, M., Ran, Y., Jansson, P.-E., Chen, P., Tan, X. and Zhang, W.: Global parameters sensitivity analysis of modeling water, energy and carbon exchange of an arid agricultural ecosystem, *Agric. For. Meteorol.*, 271, 295–306, doi:10.1016/j.agrformet.2019.03.007, 2019.

Xing, H., Wang, E., Smith, C. J., Rolston, D. and Yu, Q.: Modelling nitrous oxide and carbon dioxide emission from soil in an incubation experiment, *Geoderma*, 167–168, 328–339, doi:10.1016/j.geoderma.2011.07.003, 2011.

785 Xu, X., Thornton, P. E. and Post, W. M.: A global analysis of soil microbial biomass carbon, nitrogen and phosphorus in terrestrial ecosystems, *Glob. Ecol. Biogeogr.*, 22, 737–749, doi:10.1111/geb.12029, 2013.